

# Thermal Drawing of High-Density Macroscopic Arrays of Well-Ordered Sub-5-nm-Diameter Nanowires

Joshua J. Kaufman,<sup>†</sup> Guangming Tao,<sup>†</sup> Soroush Shabahang,<sup>†</sup> Daosheng S. Deng,<sup>‡</sup> Yoel Fink,<sup>§</sup> and Ayman F. Abouraddy<sup>\*,†</sup>

<sup>†</sup>CREOL, The College of Optics & Photonics, University of Central Florida, Orlando, Florida 32816, United States

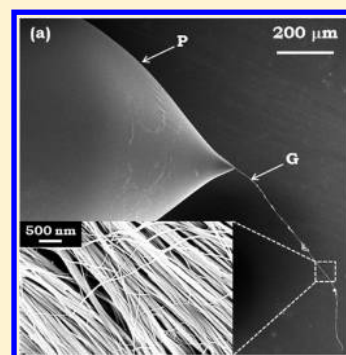
<sup>‡</sup>Department of Chemical Engineering, Massachusetts Institute of Technology, Cambridge, Massachusetts 02139, United States

<sup>§</sup>Department of Materials Science and Engineering, Massachusetts Institute of Technology, Cambridge, Massachusetts 02139, United States

**S** Supporting Information

**ABSTRACT:** We investigate the lower limit of nanowire diameters stably produced by the process of thermal fiber drawing and fiber tapering. A centimeter-scale macroscopic cylindrical preform containing the nanowire material in the core encased in a polymer scaffold cladding is thermally drawn in the viscous state to a fiber. By cascading several iterations of the process, continuous reduction of the diameter of an amorphous semiconducting chalcogenide glass is demonstrated. Starting from a 10-mm-diameter rod we thermally draw hundreds of meters of continuous sub-5-nm-diameter nanowires. Using this approach, we produce macroscopic lengths of high-density, well-ordered, globally oriented nanowire arrays.

**KEYWORDS:** nanowire synthesis, thermal fiber drawing, multimaterial fibers, nanowire arrays



Nanowire synthesis has been dominated by bottom-up approaches such as vapor–liquid–solid (VLS) growth from a catalytic droplet,<sup>1,2</sup> solution–liquid–solid growth processes,<sup>3,4</sup> and laser-ablation-assisted VLS<sup>5</sup> (see refs 6–9 for reviews). Nanowires produced in this fashion have found a wide range of applications in nanoelectronics,<sup>10</sup> energy harvesting,<sup>11</sup> photonic devices,<sup>12</sup> sensing,<sup>13</sup> and interfacing electronics with live cells.<sup>14</sup>

A seemingly unrelated fabrication technology is the top-down process of thermal fiber drawing (TFD) from a macroscopic preform.<sup>15</sup> Typically a centimeter-scale cylindrical preform is heated to the viscous state and drawn into a long length of smaller-diameter fiber while maintaining the cross-sectional geometry. Although these two techniques—bottom-up nanowire synthesis and top-down TFD—initially appear unrelated, they share the form factor of the resulting structure: a large-aspect-ratio wire. The wires produced by these distinct routes differ, however, in size and materials used. Nanowire diameters are smaller than those of optical fibers (1–100 nm for nanowires, ~10–1000 μm for typical fiber cores), have much smaller lengths (tens of micrometers for nanowires, kilometers for fibers), and are made of semiconductors<sup>16</sup> or metals,<sup>17</sup> while optical fibers are made of glassy insulators (such as silica glass<sup>18,19</sup> or polymers<sup>20</sup>).

An early prescient report<sup>21</sup> demonstrated the feasibility of using TFD to produce suspended silica microwires. Subsequent advances in photonic crystals<sup>22,23</sup> led to the development of photonic crystal fibers<sup>24–28</sup> in which the cladding consists of nanoscale-diameter filaments suspended in air and connected by

a network of thin webs. This demonstrates that TFD is capable of producing extremely long lengths (hundreds of meters) of uniform and ordered nanofilaments, albeit from glassy insulating materials. The gap in diameters between nanowires and TFD-based structures has thus narrowed considerably.<sup>29–31</sup> In a parallel development, new materials not typically associated with TFD have been recently used to produce multimaterial fibers.<sup>32</sup> Examples include photonic band gap fibers containing nanoscale multilayer structures,<sup>33,34</sup> metal–semiconductor–insulating fibers<sup>35</sup> that provide unique in-fiber optoelectronic functionality,<sup>36</sup> and TFD of crystalline silicon,<sup>37</sup> germanium,<sup>38</sup> and III–V semiconductor<sup>39</sup> cores in a silica-glass cladding.<sup>40</sup> Other approaches have produced fibers containing well-ordered arrays of microwires and nanowires of metals (500 nm diameter),<sup>41</sup> glasses,<sup>42</sup> and chalcogenides (200 nm diameter).<sup>32,43</sup> Large-length arrays of globally oriented semiconducting nanowires (200 nm diameter)<sup>44,45</sup> and filaments (100 nm wide, 10 nm thick)<sup>44</sup> have also been produced utilizing fluid instabilities<sup>46</sup> in a thin film embedded in the preform during TFD. A recent report<sup>47</sup> demonstrated nanowire and nanotube arrays produced by TFD with diameters approaching 20 nm and confirmed their continuity using the photoconductivity-measurement approach developed in ref 45.

In light of these developments in scale reduction of new materials used in TFD, an important question arises: what is the

**Received:** July 28, 2011

**Revised:** September 29, 2011

**Published:** October 03, 2011

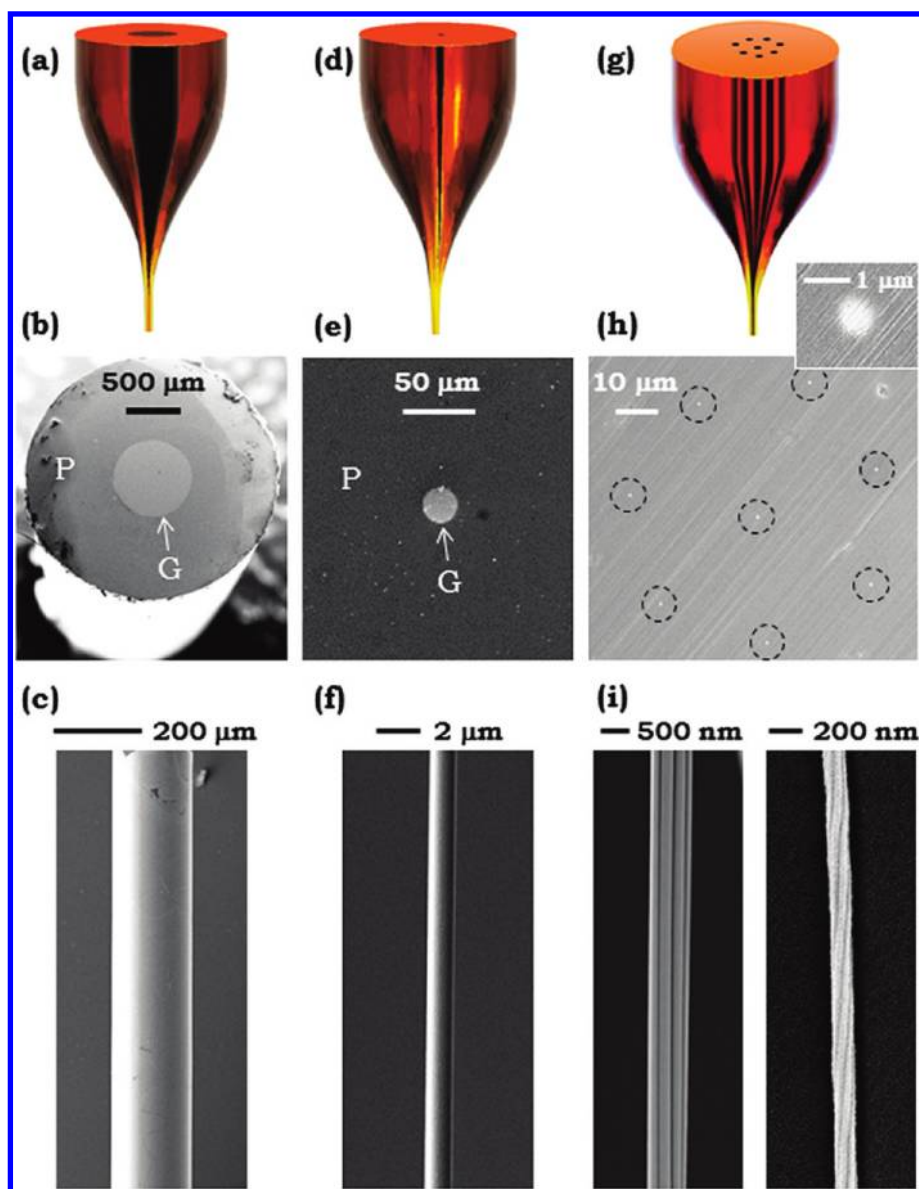


**Figure 1.** Producing in-fiber microwires and nanowires by thermal fiber drawing (TFD). (a) A first preform (the polymer is red, the glass is black), core diameter 10 mm, is drawn into a fiber; SEM micrographs of (b) a cross section (core diameter  $650\ \mu\text{m}$ ) and (c) an exposed core (diameter  $200\ \mu\text{m}$ ). (d) A second preform, containing a previously drawn fiber (from (b)) as core, is in turn drawn into a fiber; SEM micrographs of (e) a fiber cross section (core diameter  $20\ \mu\text{m}$ ) and (f) an exposed core (diameter  $1\ \mu\text{m}$ ). (g) In-fiber nanowire array produced by TFD containing an array of eight predrawn fibers. (h) SEM micrograph of a cross section. Each core ( $500\ \text{nm}$  diameter) is surrounded by a black dashed circle to guide the eye. Inset shows an individual core. (i) SEM micrographs of nanowire arrays with individual diameters  $200\ \text{nm}$  (left) and  $50\ \text{nm}$  (right).

lower limit of a feature's transverse size that may be reached by TFD while remaining axially continuous? In this paper we investigate this question in a model fiber consisting of amorphous semiconducting cores embedded in a polymer cladding. Using consecutive TFD steps, in addition to fiber tapering,<sup>48,49</sup> we successfully reduce the diameter of a semiconductor rod from 10 mm to sub-5 nm while maintaining axial continuity demonstrated by direct imaging of the nanowires after dissolving the cladding. Furthermore, we demonstrate that TFD may be used to produce globally ordered high-density arrays of nanowires extending the length of the drawn fiber. This unique approach thus imparts to nanowires the length characteristics usually associated with optical fibers. While there are several physical mechanisms that are expected to set the lower limit on axially

stable transverse feature sizes, notably fluid dynamic instabilities,<sup>46,50</sup> we have not observed the expected axial breakup in the drawn or tapered nanowires. This possibly suggests that at these nanometer scales the continuum fluid model is no longer applicable.

The fabrication of nanowires by TFD requires multiple steps of preform preparation and fiber drawing. First, we fabricate a 40-mm-diameter 10-cm-long macroscopic cylindrical preform (Figure 1a) consisting of a 10-mm-diameter amorphous semiconducting chalcogenide glass core  $\text{As}_2\text{Se}_3$  surrounded by a thermoplastic polymer cladding (polyethersulfone, PES). The two materials are thermally compatible and can be codrawn stably.<sup>29</sup> The core material is chosen from the well-known family of chalcogenide glasses that have many useful electronic<sup>32,35,36</sup>

and optical properties,<sup>51</sup> especially for mid-infrared applications,<sup>52</sup> nonlinear optics,<sup>53</sup> and phase-change memory devices.<sup>54</sup> While we demonstrate here TFD of amorphous sub-5-nm-diameter nanowires, our previous work established that post-TFD crystallization of the cores is possible via thermal treatment<sup>44,45</sup> or localized laser irradiation.<sup>45</sup> Furthermore, alternative glass compositions possess properties that allow for more controllable crystallization.<sup>55</sup>

Cascading two TFD steps, we produce a microwire embedded in a fiber. The initial 10-mm-diameter  $\text{As}_2\text{Se}_3$  rod is prepared by melt-quenching,<sup>56</sup> and the cladding is formed by rolling a  $75\ \mu\text{m}$  thick PES film followed by thermal consolidation.<sup>32</sup> The preform is then drawn in a home-built fiber draw tower (the drawing temperature is  $330\ ^\circ\text{C}$  and the drawing speed is  $1\ \text{m}/\text{min}$ ) into a fiber whose length depends on the preform dimensions and the draw-down ratio ( $10\text{--}50$  here). The typical fiber length was  $100\ \text{m}$  in our experiments. In order to examine the continuity of the semiconducting core directly, we section a length of drawn fiber and dissolve the cladding with dimethylacetamide (DMAC).<sup>44</sup> The fiber is held vertically in the solvent for  $6\ \text{h}$  to guarantee the complete removal of the polymer and release of the semiconducting core. Two core sizes produced by changing the draw-down ratio are shown in panels b and c of Figure 1 with diameters  $650$  and  $200\ \mu\text{m}$ , respectively. To further reduce the core diameter, we perform a second TFD step by placing a section of a drawn fiber in a new preform that is in turn drawn into a fiber (Figure 1d). Two cores produced in this fashion from different fibers are shown in panels e and f of Figure 1 ( $20$  and  $2\ \mu\text{m}$  diameters, respectively). We thus directly confirm the continuity, stability, and uniformity of the fiber core at the microscale.

We continue to reduce the core diameter to produce nanowires using the stack-and-draw approach,<sup>32,43,57</sup> which further yields high-density nanowire arrays. Multiple identical drawn fiber sections (eight in this case) are stacked in a new preform (Figure 1g) that is drawn into a fiber (cross section shown in Figure 1h). We span the diameter range of the individual cores from  $1\ \mu\text{m}$  to  $50\ \text{nm}$  (see Figure S3, Supporting Information) and show examples of bundles of eight  $200\text{-nm}$ - and  $50\text{-nm}$ -diameter nanowires in Figure 1i demonstrating their continuity. Although the cores in the fiber are well separated (core-to-core separation is  $> \times 30$  the core diameter; Figure 1h), the eight exposed cores adhere to each other upon removal from the DMAC solvent in an extremely orderly fashion. This spontaneously organized structure extends for the whole length of the exposed cores (several millimeters). We hypothesize that van der Waals forces are responsible for this adhesion which is initially driven by the drying of the dissolved polymer and solvent between the strands. The effect is repeatable, reproducible, and quite robust. The smallest-diameter bundle (individual core diameter  $\sim 50\ \text{nm}$ , Figure 1i) is helically twisted along its whole length, which we do not readily observe in the larger-diameter bundles. The twisting appears to occur after removing the nanowires from the solvent, likely due to transverse perturbing forces.

Several advantageous features are provided by TFD when viewed as a top-down approach to nanowire fabrication. First, the process is scalable, i.e., a large number of cores may be produced simultaneously in a single fiber through the stack-and-draw process. For example, a  $1\text{-mm}$ -diameter fiber may potentially include  $10^7$   $100\text{-nm}$ -diameter nanowires. Second, TFD produces extremely long nanowires that are limited, in principle, by the drawn fiber length. Third, global order and orientation are

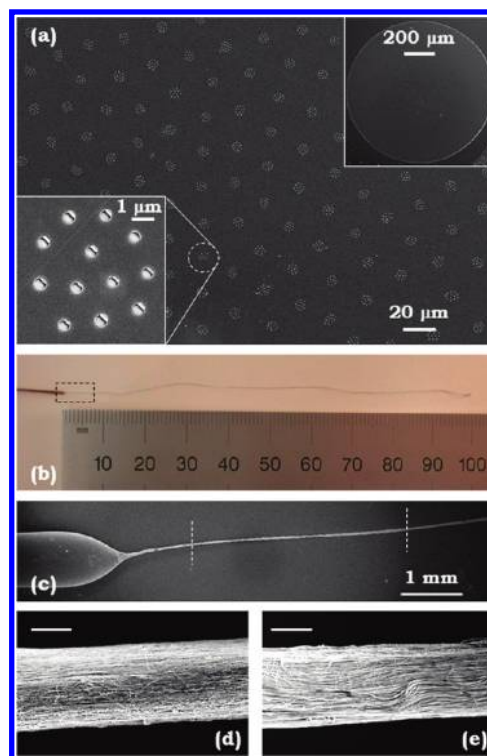


**Figure 2.** High-density arrays of  $500\text{-nm}$  and  $200\text{-nm}$ -diameter wires. (a) SEM image of a well-ordered array of  $\sim 330$  nanowire bundles, each bundle consisting of  $12$   $500\text{-nm}$ -diameter semiconducting glass cores embedded in a polymer cladding. Top-right inset is an SEM of the full fiber cross section, and bottom-left inset is an SEM of a single bundle. For preform fabrication, see Supporting Information (Figure S1). (b) A photograph of an exposed  $10\ \text{cm}$  long bundle of  $\sim 27000$   $200\text{-nm}$ -diameter nanowires emerging from the fiber tip after dissolving the polymer cladding. (c) SEM micrograph of the dashed box in (b). (d) and (e) show SEM micrographs taken along the bundle in (c) at the locations marked by dashed white vertical lines. The scale bars in (d) and (e) are both  $20\ \mu\text{m}$ .

imposed on the fabricated nanowire array at the preform level during the stacking process. The polymer scaffold offers mechanical support to the nanowire array and provides electrical insulation between the individual nanowires. In comparison to previous work on top-down nanowire fabrication, such as lithographic templates<sup>58</sup> or pattern transfer,<sup>59</sup> TFD allows for simpler production of extremely long well-ordered nanowire arrays.

These features are all demonstrated in Figure 2. A large number of fibers ( $\sim 330$ ), each containing  $12$   $20\text{-}\mu\text{m}$ -core-diameter fibers, are stacked in a preform and drawn into a fiber containing  $\sim 4000$   $500\text{-nm}$ -diameter cores (Figure 2a; see Figure S2 in the Supporting Information). The array of stacked fibers retains its arrangement in the newly drawn fiber, and the  $12$  cores in each lattice site also retain their pre-TFD arrangement. Another preform was produced by stacking  $\sim 330$  fibers each containing  $80$   $7\text{-}\mu\text{m}$ -diameter cores and was then drawn into a fiber. By dissolving the cladding, we expose a  $10\ \text{cm}$  long bundle of  $\sim 27000$  ( $\sim 80 \times 330$ )  $200\text{-nm}$ -diameter wires (Figure 2b) demonstrating the macroscopic stability and continuity of the nanowire array. This is further confirmed by SEM micrographs taken along the exposed bundle (Figure 3 panels c–e). We demonstrate the control over nanowire size in panels a–c of Figure 3 where we produce high-density, globally oriented arrays

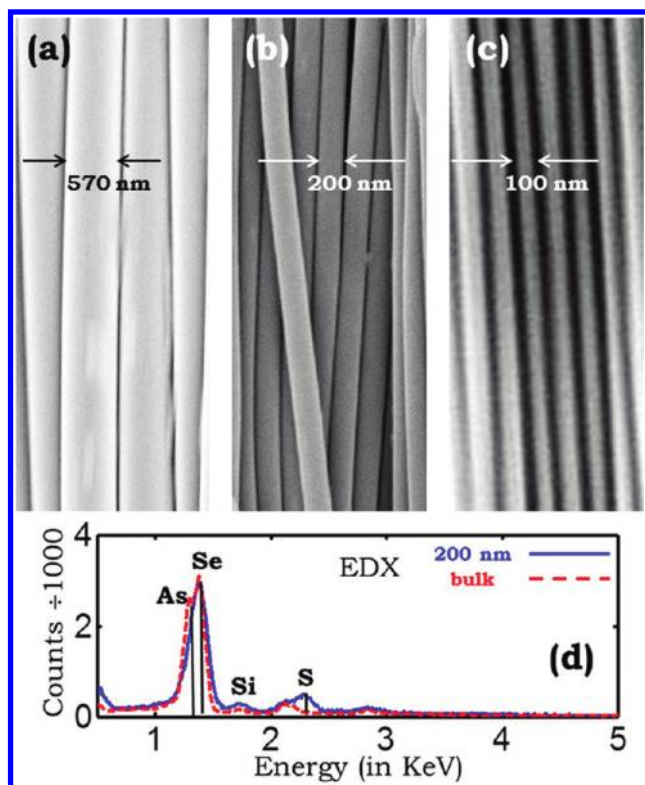


**Figure 3.** (a–c) SEM micrographs of ordered nanowire arrays after removal of the polymer cladding. The nanowire diameters are (a) 570, (b) 200, and (c) 100 nm. (d) EDX of the nanowire bundle (continuous blue line) and the bulk glass (dashed red line) obtained in the SEM showing an elemental decomposition compatible with the material  $\text{As}_2\text{Se}_3$ . The sulfur peak in the nanowire EDX is due to remnant PES polymer.

with nanowire diameters of 570, 200, and 100 nm, respectively. An energy-dispersive X-ray spectroscopy (EDX) measurement of the 200-nm-diameter nanowire bundle (Figure 3d) is compatible with the hypothesis that the bundle consists solely of  $\text{As}_2\text{Se}_3$  with almost complete elimination of the polymer. We compare the EDX of the nanowires with that of the bulk glass in Figure 3d and observe no change in the composition of the glass in the two forms (bulk and nanowires). Note that the sulfur peak in the nanowires (due to remnant polymer PES which contains sulfur) is not observed in the case of the bulk glass (which does not contain sulfur). We do not observe here any signs of breakup, irregularities, or discontinuities in all of the above examples of nanowires produced by TFD or tapering in Figures 1–3, with diameters extending from 650  $\mu\text{m}$  to 50 nm.

In order to investigate the lower limit of this process, we use another stack-and-draw step that reduces the nanowire diameters to 20 nm and, subsequently, use fiber tapering to reach 5 and 2.5 nm. We stack 80 fibers each containing  $\sim 4000$  500-nm-diameter cores in a preform drawn into a fiber. After dissolving the cladding, we are left with continuous cores as shown in Figure 4a. By isolating single strands of the exposed cores, we confirm the continuity of the 20 nm nanowires using both SEM (Figure 4b) and TEM (Figure 4c) imaging (JEOL JEM-1011 TEM). Note that a thin polymer film remains connecting pairs of nanowires. Since we did not observe any signs of nanowire disintegration, we further reduce the core sizes.

Further size reduction is achieved by fiber tapering<sup>48,49</sup> (Figure 5a). In the tapering procedure, the fiber temperature is

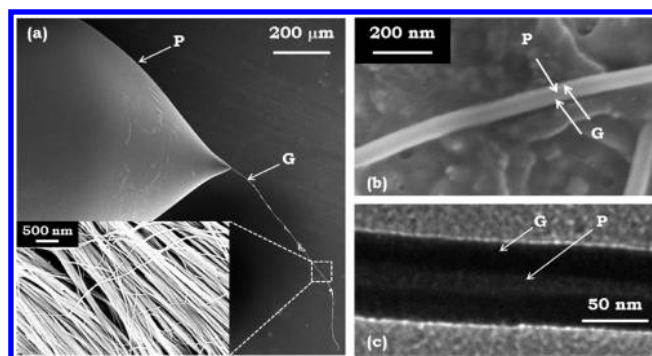


**Figure 4.** High-density array of 20-nm-diameter nanowires. (a) SEM micrograph of the fiber tip showing the nanowire bundle after removing the polymer. The inset shows a higher-resolution SEM micrograph revealing the nanowires in the bundle. (b) SEM micrograph of a pair of 20-nm-diameter nanowires, isolated from the inset in (a), connected by a thin polymer web not removed by the solvent. (c) TEM micrograph of the nanowire pair in (b) allowing accurate measurement of the nanowire diameter.

locally elevated in a heating zone (length  $\sim 7.5$  mm, the tapering temperature is 291  $^\circ\text{C}$ , and the tapering speed is 2–3 mm/s) to reduce the material viscosity. The fiber is then pulled symmetrically from both ends thus controllably reducing the diameter in the heating zone. We first reduce this fiber diameter by a factor of 4, such that the resulting individual nanowires are expected to have  $\sim 5$  nm diameter. Figure 5b highlights the continuity of the exposed nanowire bundle after dissolving the polymer cladding. High-resolution SEM imaging (Figure 5c–e) confirms the continuity of the core nanowires and the global orientation of the exposed nanowire bundle. Tapering the fiber in Figure 4 by a factor of 8 produces  $\sim 2.5$ -nm-diameter nanowires, and the continuity of the cores is also confirmed after dissolving the cladding (see Figure S4 in the Supporting Information). Note that the material viscosity during fiber tapering is lower than during TFD (because of the smaller volume of the fiber compared to the preform) and hence capillary instability is more likely to initiate during tapering.<sup>59</sup> Since the sub-5-nm-diameter nanowires survive the tapering procedure, they are also highly likely to survive TFD.

We accurately determine the diameter of the nanowires produced by tapering by TEM imaging. We section a thin slice of the fiber tip (without dissolving the cladding, Figure 5f-i) using a microtome (Leica EM UC7 Ultramicrotome, diamond blade). The polymer slice is less than 200 nm thick, has  $\sim 250$ - $\mu\text{m}$  diameter (after tapering a 1-mm-outer-diameter fiber by a factor of 4), and contains well-separated nanowire bundles, each bundle containing 12 nanowires embedded in the polymer matrix. The slice is placed on a TEM grid (Figure 5f-ii) and immersed in DMAC to dissolve the polymer. The grid is removed from the solution after 2 h and is allowed to dry in air before being used in the TEM (Figure 5f-iii). We find on the grid multiple separated bundles of short nanowire sections as expected from the original fabricated fiber structure (Figure 3a) used in the subsequent stack-and-draw steps. A typical bundle is shown in Figure 5g and the TEM image confirms the sub-5-nm diameters expected from the tapering ratio. An EDX measurement of the nanowire bundle obtained while it is still encased in the polymer slice (Figure 5f-ii) using a high-resolution TEM (FEI Technai F30 TEM) confirms that  $\text{As}_2\text{Se}_3$  is present in the bundle (Figure 5h). The elemental

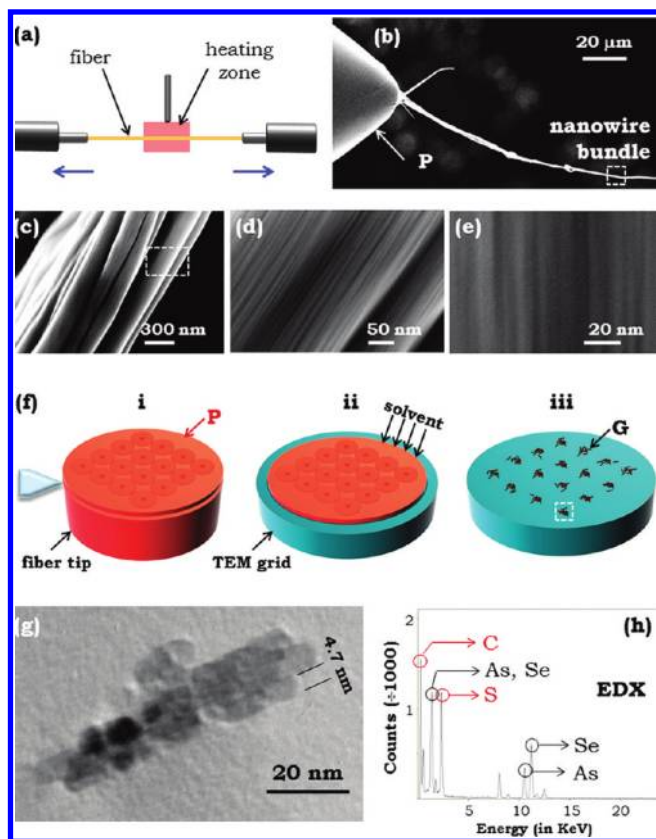


**Figure 5.** Producing sub-5-nm-diameter nanowires by fiber tapering. (a) Simplified schematic of the fiber tapering setup. (b) SEM micrograph of an intact exposed bundle of 5-nm-diameter nanowires emerging from the tapered fiber tip. (c) SEM micrograph of the dashed white box in (b), and (d) a zoomed-in SEM micrograph of the dashed white box in (c), both showing continuous bundles of nanowires. (e) High-resolution SEM micrograph of a section in (d). (f) TEM sample preparation: i, a thin slice is sectioned from the fiber tip using a microtome diamond blade; ii, the slice is placed on a TEM grid and a solvent dissolves the polymer, P; iii, well-separated bundles of 12 5-nm-diameter nanowires, G, less than 200 nm long. (g) TEM micrograph of a short bundle of 5-nm-diameter nanowires corresponding to the white dashed box in (f, iii). (h) EDX of the nanowires obtained using the TEM showing an elemental composition compatible with the nanowire material  $\text{As}_2\text{Se}_3$  (black-colored elements) and remnants of the polymer PES (red-colored elements).

composition of PES is also observed in Figure 5h since the polymer was not dissolved, compared to Figure 3d where the polymer was completely removed before the EDX measurement. The outer diameter of the tapered fiber containing 2.5-nm-diameter nanowires was too small for the preparation of a thin slice using the microtome and TEM imaging was consequently not performed.

We have thus confirmed that the nanowires produced by TFD and tapering to sub-5-nm diameters are axially continuous for macroscopic lengths. This result is remarkable in light of the various breakup mechanisms that are expected to limit transverse feature sizes that remain axially continuous. Paramount among these factors is capillary fluid instabilities.<sup>46,50</sup> During TFD and tapering processes, the cores are melted into a viscous fluid surrounded by the viscous polymer matrix. The wires are thus subject to the classical Plateau–Rayleigh capillary instability<sup>50</sup> and are consequently anticipated to break up into droplets which

we have previously observed at the microscale under well-controlled conditions.<sup>60</sup> As the core diameter is further reduced to 5 nm, the capillary instability time becomes smaller and the nanowires are more susceptible to instability according to the classical Tomotika model.<sup>61</sup> However, we find that the wires are unexpectedly stable during tapering (at temperature 291 °C, tapering time  $\sim 2$  s, and tapering speed 3–4 mm/s) to sub-3-nm-diameter. This stability, and the apparent suppression of capillary instabilities, is not yet fully understood. There are several potential hypotheses for the discrepancy between the expected breakup and the observed continuity of the nanowires. First, at these nanometer scales the continuum limit that is a prerequisite for the validity of fluid dynamic models may no longer apply. Second, the close proximity of the nanowires in the polymer matrix may result in coupling between adjacent nanowires that suppresses the growth of capillary instabilities. This is a departure from the Tomotika model<sup>61</sup> (and earlier Rayleigh models<sup>62</sup>) that assumes an infinite fluid cladding surrounding the inner fluid. Furthermore, the complicated TFD process may give rise to other factors, beyond the scope of this paper, that may contribute to the stability of these extremely long nanowires.<sup>46</sup>

In conclusion, we have demonstrated that thermal fiber drawing and fiber tapering may be used to draw amorphous semiconducting nanowires to sub-5-nm diameters while maintaining axial continuity during TFD or subsequent tapering processes. Extremely long lengths of high-density, globally oriented and ordered arrays of these nanowires are combined in a single fiber. Such nanowire arrays are expected to find applications in nanosensing, nanoimaging using nanowire tips, and energy harvesting. The robustness of the nanowire bundles and their encasement in a polymer matrix scaffold further suggest important applications in live cell bioprobng.

## ■ ASSOCIATED CONTENT

**S** Supporting Information. Figure S1, preform fabrication; Figure S2, stack-and-draw fabrication of a high-density, well-ordered nanowire array; Figure S3, SEM micrograph of exposed nanowire bundles with diameters from 1  $\mu\text{m}$  down to 50 nm; and Figure S4, SEM micrographs of an exposed high-density bundle of 2.5-nm-diameter nanowires. This material is available free of charge via the Internet at <http://pubs.acs.org>.

## ■ AUTHOR INFORMATION

### Corresponding Author

\*E-mail: raddy@creol.ucf.edu.

## ■ ACKNOWLEDGMENT

This work was funded by the NSF (ECCS-1002295), the ORAU (Ralph E. Powe Junior Faculty Enhancement Award), and CREOL, The College of Optics & Photonics (UCF). We thank P. H. Prideaux and E.-H. Banaei for technical assistance and M. Z. Bazant, M. J. Soileau, and Bahaa E. A. Saleh for their encouragement and support.

## ■ REFERENCES

- (1) Wagner, R. S.; Ellis, W. C. *Appl. Phys. Lett.* **1964**, *4*, 89.
- (2) *Whisker Technology*; Levitt, A. P., Ed.; Wiley-Interscience: New York, 1970.

- (3) Trentler, T. J.; Hickman, K. M.; Goel, S. C.; Viano, A. M.; Gibbons, P. C.; Buhro, W. E. *Science* **1995**, *270*, 1791.
- (4) Holmes, J. D.; Johnston, K. P.; Doty, R. C.; Korgel, B. A. *Science* **2000**, *287*, 1471.
- (5) Morales, A. M.; Lieber, C. M. *Science* **1998**, *279*, 208.
- (6) Hu, J.; Odom, T. W.; Lieber, C. M. *Acc. Chem. Res.* **1999**, *32*, 435.
- (7) Xia, Y.; Yang, P.; Sun, Y.; Wu, Y.; Mayers, B.; Gates, B.; Yin, Y.; Kim, F.; Yan, H. *Adv. Mater.* **2003**, *15*, 353.
- (8) Law, M.; Goldberger, J.; Yang, P. *Annu. Rev. Mater. Res.* **2004**, *34*, 83.
- (9) Yang, P.; Yan, R.; Fardy, M. *Nano Lett.* **2010**, *10*, 1529.
- (10) Yan, H.; Choe, H. S.; Nam, S. W.; Hu, Y.; Das, S.; Klemic, J. F.; Ellenbogen, J. C.; Lieber, C. M. *Nature* **2011**, *470*, 240.
- (11) Hochbaum, A. I.; Yang, P. *Chem. Rev.* **2010**, *110*, 527.
- (12) Yan, R.; Gargas, D.; Yang, P. *Nat. Photonics* **2009**, *3*, 569.
- (13) Yang, F.; Kung, S.-C.; Cheng, M.; Hemminger, J. C.; Penner, R. M. *ACS Nano* **2010**, *4*, 5233.
- (14) Timko, B. P.; Cohen-Karni, T.; Qing, Q.; Tian, B.; Lieber, C. M. *IEEE Trans. Nanotechnol.* **2010**, *9*, 269.
- (15) *Optical Fiber Communications, Vol. 1: Fiber Fabrication*; Li, T., Ed.; Academic Press: Orlando, FL, 1985.
- (16) Duan, X.; Lieber, C. M. *Adv. Mater.* **2000**, *12*, 298.
- (17) Zach, M.; Ng, K.; Penner, R. M. *Science* **2000**, *290*, 2120.
- (18) Maurer, R. D.; Schultz, P. C. US patent 3,659,915, 1972.
- (19) Keck, D. B.; Maurer, R. D.; Schultz, P. C. *Appl. Phys. Lett.* **1973**, *22*, 307.
- (20) Kuzyk, M. G. *Polymer Fiber Optics: Materials, Physics, and Applications*; CRC Press: Boca Raton, FL, 2007.
- (21) Kaiser, P.; Marcattili, E. A. J.; Miller, S. E. *Bell Syst. Tech. J.* **1973**, *52*, 265.
- (22) Yablonovitch, E. *Phys. Rev. Lett.* **1987**, *58*, 2059.
- (23) Joannopoulos, J. D.; Johnson, S. G.; Winn, J. N.; Meade, R. D. *Photonic Crystals: Molding the Flow of Light*, 2nd ed.; Princeton University Press: Princeton, NJ, 2008.
- (24) Knight, J. C.; Birks, T. A.; Russell, P. St. J.; Atkin, D. M. *Opt. Lett.* **1996**, *21*, 1547.
- (25) Birks, T. A.; Knight, J. C.; Russell, P. S. *Opt. Lett.* **1997**, *22*, 961.
- (26) Cregan, R. F.; Mangan, B. J.; Knight, J. C.; Birks, T. A.; Russell, P. St. J.; Roberts, P. J.; Allan, D. C. *Science* **1999**, *285*, 1537.
- (27) Knight, J. C. *Nature* **2003**, *424*, 847.
- (28) Russell, P. *Science* **2003**, *299*, 358.
- (29) Tong, L.; Lou, J.; Ye, Z.; Svacha, G. T.; Mazur, E. *Nanotechnology* **2005**, *16*, 1445.
- (30) Brambilla, G.; Xu, F.; Feng, X. *Electron. Lett.* **2006**, *42*, 517.
- (31) Chuo, S.-M.; Wan, M.-H.; Wang, L. A.; Wang, J.-S. *J. Lightwave Technol.* **2009**, *27*, 2983.
- (32) Abouraddy, A. F.; Bayindir, M.; Benoit, G.; Hart, S. D.; Kuriki, K.; Orf, N.; Shapira, O.; Sorin, F.; Temelkuran, B.; Fink, Y. *Nat. Mater.* **2007**, *6*, 336.
- (33) Temelkuran, B.; Hart, S. D.; Benoit, G.; Joannopoulos, J. D.; Fink, Y. *Nature* **2002**, *420*, 650.
- (34) Benoit, G.; Hart, S. D.; Temelkuran, B.; Joannopoulos, J. D.; Fink, Y. *Adv. Mater.* **2003**, *15*, 2053.
- (35) Bayindir, M.; Sorin, F.; Abouraddy, A. F.; Viens, J.; Hart, S. D.; Joannopoulos, J. D.; Fink, Y. *Nature* **2004**, *431*, 826.
- (36) Abouraddy, A. F.; Shapira, O.; Bayindir, M.; Arnold, J.; Sorin, F.; Hinczewski, D. S.; Joannopoulos, J. D.; Fink, Y. *Nat. Mater.* **2006**, *5*, 532.
- (37) Ballato, J.; Hawkins, T.; Foy, P.; Stolen, R.; Kokuoz, B.; Ellison, M.; McMillen, C.; Reppert, J.; Rao, A. M.; Daw, M.; Sharma, S. R.; Shori, R.; Stafsudd, O.; Rice, R. R.; Powers, D. R. *Opt. Express* **2008**, *16*, 18675.
- (38) Ballato, J.; Hawkins, T.; Foy, P.; Morris, S.; Hon, N. K.; Jalali, B.; Rice, R. *Opt. Lett.* **2011**, *36*, 687.
- (39) Ballato, J.; Hawkins, T.; Foy, P.; McMillen, C.; Burka, L.; Reppert, J.; Podila, R.; Rao, A. M.; Rice, R. R. *Opt. Express* **2010**, *18*, 4972.
- (40) Ballato, J.; Hawkins, T.; Foy, P.; Yazgan-Kokuoz, B.; McMillen, C.; Burka, L.; Morris, S.; Stolen, R.; Rice, R. *Opt. Fiber Technol.* **2010**, *16*, 399.
- (41) Zhang, X.; Ma, Z.; Yuan, Z.-Y.; Su, M. *Adv. Mater.* **2008**, *20*, 1310.
- (42) Ma, Z.; Ma, L.; Su, M. *Adv. Mater.* **2008**, *20*, 3734.
- (43) Bayindir, M.; Abouraddy, A. F.; Shapira, O.; Viens, J.; Saygin-Hinczewski, D.; Sorin, F.; Arnold, J.; Joannopoulos, J. D.; Fink, Y. *IEEE J. Sel. Top. Quantum Electron.* **2006**, *12*, 1202.
- (44) Deng, D. S.; Orf, N. D.; Abouraddy, A. F.; Stolyarov, A. M.; Joannopoulos, J. D.; Stone, H. A.; Fink, Y. *Nano Lett.* **2008**, *8*, 4265.
- (45) Deng, D. S.; Orf, N. D.; Danto, S.; Abouraddy, A. F.; Joannopoulos, J. D.; Fink, Y. *Appl. Phys. Lett.* **2010**, *96*, 023102.
- (46) Deng, D. S.; Nave, J.-C.; Liang, X.; Johnson, S. G.; Fink, Y. *Opt. Express* **2011**, *19*, 16273.
- (47) Yaman, M.; Khudiyev, T.; Ozgur, E.; Kanik, M.; Aktas, O.; Ozgur, E. O.; Deniz, H.; Korkut, E.; Bayindir, M. *Nat. Mater.* **2011**, *10*, 494.
- (48) Birks, T. A.; Li, Y. W. *J. Lightwave Technol.* **1992**, *10*, 432.
- (49) Tong, L.; Gattass, R. R.; Ashcom, J. B.; He, S.; Lou, J.; Shen, M.; Maxwell, I.; Mazur, E. *Nature* **2003**, *426*, 816.
- (50) Eggers, J.; Villermaux, E. *Rep. Prog. Phys.* **2008**, *71*, 036601.
- (51) Hilton, A. R. *J. Non-Cryst. Solids* **1970**, *2*, 28.
- (52) Sanghera, J. S.; Shaw, L. B.; Aggarwal, I. D. *IEEE J. Sel. Top. Quantum Electron.* **2009**, *15*, 114.
- (53) Zakery, A.; Elliott, S. R. *Optical Nonlinearities in Chalcogenide Glasses and their Applications*; Springer-Verlag: Berlin, 2007.
- (54) Hudgens, S.; Johnson, B. *MRS Bull.* **2004**, *29*, 829.
- (55) Calvez, L.; Ma, H. L.; Lucas, J.; Zhang, X. H. *Adv. Mater.* **2006**, *19*, 129.
- (56) Hilton, A. R. *Appl. Opt.* **1966**, *5*, 1877.
- (57) Russell, P. St. J. *J. Lightwave Technol.* **2006**, *24*, 4729.
- (58) Menke, E. J.; Thompson, M. A.; Xiang, C.; Yang, L. C.; Penner, R. M. *Nat. Mater.* **2006**, *5*, 914.
- (59) Boukai, A. I.; Bunimovich, Y.; Tahir-Kheli, J.; Yu, J.-K.; Goddard, W. A., III; Heath, J. R. *Nature* **2008**, *451*, 168.
- (60) Shabahang, S.; Kaufman, J. J.; Deng, D. S.; Abouraddy, A. F. *Appl. Phys. Lett.* **2011** in press.
- (61) Tomotika, S. *Proc. R. Soc. London, Ser. A* **1935**, *150*, 322.
- (62) Rayleigh, L. *Philos. Mag.* **1892**, *34*, 145.